Supplementary Information

A. MRI Method

During MRI, the animal was anaesthetized using 3% (+/- 1%) isoflurane in oxygen and received an intraperitoneal injection of sterile saline (3ml) to avoid dehydration during the procedure. Throughout the entire procedure, a mixture of oxygen and 2% (+/- 0.5%) isoflurane was administered to maintain anesthesia. A custom-made head holder (Qualita Ltd., Saitama, Japan) was used to fix the marmoset head within the imaging tube, such that the rostral-caudal axis of the head was stereotaxically aligned with the tube. A small glass capillary with a contrast agent was used in each ear bar, such that the positions of the ear bars would be visible in the MRI images. A heating pad was used to maintain the body temperature. Heart rate, blood oxygen saturation levels, rectal temperature and respiration rate were continuously monitored and recorded every 10 minutes.

During ***in-vivo*** **MR** imaging, high-resolution 3D T1 mapping was carried out using a Magnetization-Prepared Rapid Gradient-Echo (MPRAGE) sequence [1] with a repetition time (TR) = 6000 ms, inversion times (TI) = 150, 1300, 4000 ms, (TE (echo time) = 2 ms TD (time-domain) = 9 ms) and a nominal flip angle (FA) = 12 degrees. Imaging planes were axial slices with FOV = 48.0×38.4×22.6 mm at matrix size = 178×142×42. T2-weighted images (T2WI) were acquired using a rapid acquisition with relaxation enhancement sequence [2] with the following parameters: repetition time/echo time echo = 4000 ms/22.0 ms, RARE factor = 4, averages = 3, field of view = 48 mm × 48 mm, matrix = 178 × 178, slice thickness = 0.54 mm.

Diffusion weighted images were acquired by a pulse-field gradient spin-echo (PGSE, the Stejskal-Tanner diffusion preparation (Stejskal & Tanner, 1965)) based on echo planner imaging sequences along 30 MPG axes and were acquired with the following parameters: b-values = 1000 s/mm^2, TR = 4000 ms, TE = 25.57 ms, averages = 3, k-space segments = 6, matrix = 128 x 128, FOV = 44.8 x 44.8 mm^2, and slice thickness = 0.7 mm. The DTI map was acquired using a method adapted from Fujiyoshi et al. [3]. An eigenvector associated with the largest eigenvalue λ1 was assumed to represent the local fiber direction. Three DTI maps were reconstructed from the data as follows: axial diffusivity (AD) = λ1, radial diffusivity (RD) = (λ2 + λ3)/2, and mean diffusivity (MD) = (λ1 + λ2 + λ3)/3.

For the ***ex-vivo*** **MR** imaging following perfusion, the brain was immersed in an electronic liquid (Fluorinert FC-72; 3M) in a 32 mm ID acrylic tube. High resolution T2-weighted images (T2WI) were acquired using a rapid acquisition with relaxation enhancement sequence [4] with the following parameters: repetition time/echo time echo = 10000 ms/29.36 ms, RARE factor = 4, averages = 16, field of view = 36 mm × 30 mm, matrix = 360 × 300, slice thickness = 0.2 mm. Diffusion weighted images were acquired by a pulse-field gradient spin-echo (PGSE, the Stejskal-Tanner diffusion preparation (Stejskal & Tanner, 1965)) based echo planner imaging [5] sequence along 128 MPG axes which was acquired with the following parameters: b-values = 1000, 3000 and 5000 s/mm^2, TR = 4000 ms,

TE = 28.4 ms, averages = 2, k-space segments = 10, matrix = 190 x 190, FOV = 38.0 x 38.0 mm^2, and slice thickness = 0.2 mm.

B. Tracer Injections

Our project plans to cover ~400 injection sites in the marmoset brain, one anterograde and one retrograde tracer at each site, evenly distributed across the grey matter of the right hemisphere of the marmoset brain. The stereotaxic coordinates of all injection sites were systematically chosen using an MRI-based atlas [6] and the injection location choice was based on an established algorithm [7]. Briefly, the right hemisphere was separated into 400 equal sized parcels, respecting anatomical boundaries. The plan resulted in 297 injection sites within the cerebral cortex, and 103 injection sites in the subcortical regions. Each subcortical region was evaluated in terms of the structure's volume. The injection was then placed based on the grid space modeled for the individual structure of interest.

We used a borosilicate micropipette with an outer diameter of 20-30µm as a vector of injection. The tracer was placed at each appropriate depth with an injection speed of 20µl/min. Anterograde tracers, AAVTRE3TdTom (0.3 µl) and AAVTRE3Clover (0.3 µl) and retrograde tracers, Fast Blue (FB, 0.3 µl 5% solution in distilled water; Funakoshi; Tokyo, Japan) and biotin conjugated Cholera toxin subunit B (CTB, 0.6 µl 1% Enzolife, New York, USA) were used.

Post recovery, the animal was housed individually and monitored throughout the 4-week incubation period. The animal received a non-steroidal anti-inflammatory (Oral Metacam; 0.05 mg/kg, Boeringer Ingelheim) for three days immediately following the surgery.

C. Perfusion/Embedding

After the 4-week viral incubation period, the animal was euthanized and perfused. The marmoset was injected with Diazepam (Pamlin:2mg/kg), Ketamine (10mg/kg), then pentobarbital (80mg/kg) to anesthetize. The animal was then perfused using an 18" oral gavage needle that entered the left ventricle and terminated at the aorta through the aortic valve. 500mL of heparinised PBS was used (50ml/min) to remove the blood supply prior to the beginning of asystole to ensure that no clotting occurred; afterwards 500mL of 4% PFA in 0.1M PB was used (70ml/min) for fixation purposes.

After extraction, the brain was submerged in 4% PFA overnight. The brain was then transferred to 0.1M PB and underwent a post-mortem *ex-viv*o MRI. Following the *ex-vivo* MRI, the brain was transferred into 10% sucrose in 0.1M PB overnight and then placed in 30% sucrose in 0.1M PB for means of temperature protection.

A rectangular base mold was custom made with Polylactic Acid (PLA) at 3x4x5 mm. A slit was opened from the bottom of the mold and an additional piece of PLA was cut to fit into the slit for easy removal of the brain block after the freezing process. A 3D-printed brain mold made from MR images of several marmoset brains [6] was attached to a

positioning bar with its rostral side facing the arrow direction (Figure 1). A custom freezing platform, also 3D-printed, secured the base mold flat and allowed the positioning bar for the brain mold (dorsal side down) to adjust vertically.

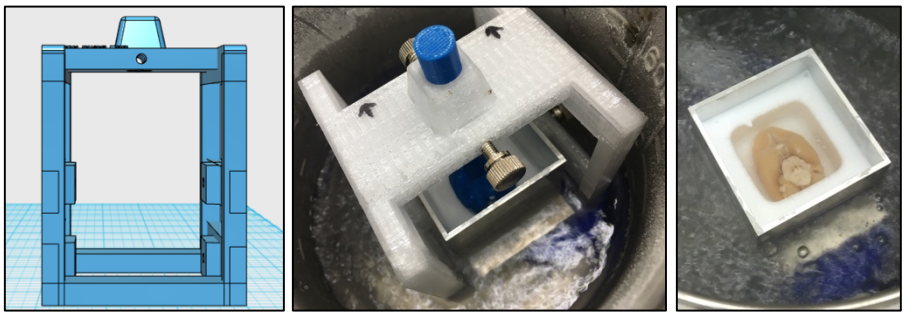

Figure 1. Rectangular base mold was designed and printed to serve as a freezing platform. The freezing platform was used to control the position of the brain mold to the base mold during freezing. The positioning bar is adjustable to allow ease of insertion and removal of the brain mold from the base mold.

While the brain and base molds were attached to the freezing platform, the positioning bar was adjusted to lower the brain mold dorsal (down) side to 2 mm from the slit. Embedding medium Neg50 (Richard Allen Scientific, Waltham, MA) was then added into the base mold until it slightly touched the dorsal (down) side of the brain mold. The freezing platform, with the base and brain mold still attached, was placed in a -80 ^{o}C freezer until the Neg50 was solid.

When the Neg50 was fully frozen, the brain mold was briefly thawed by a heat gun to remove it from the base mold. The surface temperature of the brain mold cavity was kept at -2 ^{o}C to hold the brain shape while leaving the Neg50 solid. Additional Neg50 was then added to the base mold, filled to a volume to sufficiently immerse the brain, and left to thermally stabilize for 15 seconds. The brain was removed from the 30% sucrose in 0.1M PB solution and dried for 30-45 seconds before being carefully placed within the Neg50 filled base mold with the ventral side of the brain facing up at a 0^{o} horizontal plane. The base mold was then placed in dry-ice chilled 2-methylbutane until all the Neg50 was uniformly frozen. Finally, the base mold was thawed by a heat gun to remove the brain block from the base mold apparatus, placed in a properly labeled freezer bag, and stored in a -80 ^{o}C freezer.

D. Cryo-sectioning

The cryostat's stage was modified to accommodate the larger dimensions of a cryo-embedded brain block and aided in stabilizing the cryostat's chuck and blade (Figure 2a and 3b). The UV-LED device was arranged in 4 rows of 11 LEDs in a parallel resistor network to provide uniform UV intensity across the surface of the slides. Each array was connected to a single 6V DC power source and regulated by an on-off timer controller using a Raspberry Pi [8]. Figure 2c shows the setup of the UV station within the cryostat.

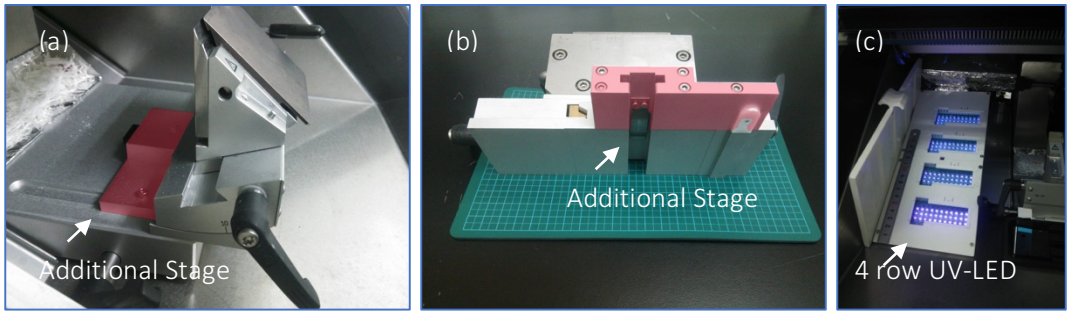

Figure 2. (a,b) Additional stage shown in pink was attached to the original cryostat stage to increase the room space and to aid in stabilization of the cryostats chuck and blade. (c) a 4 row UV-LED device to provide UV intensity across the surface of the slides by an on-off timer controller using a Raspberry Pi.

E. Histology (Staining)

The slides for **Nissl** staining were processed through an automated Nissl staining protocol beginning with a thionin solution: 1.88g thionin chloride (TCI, T0214) in 750mL De-ionized H_2O (DiH_2O), 9mL of glacial acetic acid (WAKO, 012-00245), and 1.08g sodium hydroxide pellets (Sigma-Aldrich, 221465-500G). The slides then underwent three washes of DiH_2O followed by dehydration in increasing concentrations of ethanol 50%, 70%, 95% 100% and finally Xylene, [9,10] followed by automatic cover-slipping.

The **myelin** staining technique used a modified ammoniacial silver impregnation technique originally developed by Gallyas [11]. Instead of the standard protocol of implementing the technique on free floating sections, the protocol was applied to the slide mounted sections. After the physical development of the myelin stain, the tissue was manually inspected for staining and morphological quality. The slides were then put on a drying rack for 24 hours and were dehydrated with ethanol followed by automatic cover-slipping.

The **CTB** designated slides were manually loaded into Immunohistochemistry (IHC) basins (Light Labs, LM920-1). The basins were filled to ½ of their volume with tap water to maintain humidity levels. In our CTB-DAB (3,3'diaminobenzidine) protocol , the solutions were pipetted with ~800uL onto each slide. The first step, blocking, consisted of 15 mL methanol (Nacalai Tesque, 21915-35), 480mL 1xPBS, and 1.25mL hydrogen peroxide H_2O_2 (Wako, 081-04215) was shaken and sprayed onto the slides. The protein block was made of 1% v/v triton X-100 (Sigma Aldrich, X100-500G), 3.5% v/v normal rabbit serum (Vector Labs, S-5000) in 1xPBS for 30 minutes at room temperature (RT), followed by 1xPBS rinse 3 times and pressure assisted drying. The primary antibody step consisted of 2% v/v goat anti-CTB (List Laboratories, #703) (1:2500 concentration), 0.3% v/v triton X-100, 3% v/v normal rabbit serum in 1xPBS which was left overnight at RT with the IHC basins covered to preserve liquid levels and ambient humidity within the basin. Once the slides went through a 1xPBS rinse 3 times and pressure assisted drying, the secondary antibody made up of 0.4% v/v biotinylated rabbit-anti-goat IgG (H+L) (Vector Labs, BA-5000) (1:250 concentration), 1% v/v normal rabbit serum, 0.3% v/v triton X-100 in 1xPBS was added and left for two hours at RT. After another 1xPBS rinse 3 times and dry cycle the Avidin-biotin complex elite kit (ABC, Vector Labs, VEC-PK-6100) was placed on the slides and left to incubate for three hours at RT. The ABC kit was

used with equal volumes of avidin and biotin, 1% v/v avidin and biotin were made 30 minutes before use.

Our DAB-Nickel Cobalt (DAB-NiCo) staining protocol used 1% w/v DAB (Apollo Scientific Limited, BID2042) 1% w/v ammonium nickel (II) sulfate hexahydrate (Santa Cruz Biotechnology, sc-239235), 1% w/v Cobalt (II) Chloride hexahydrate (Sigma Aldrich, 255599-500G), and 0.00003% v/v H_2O_2. The DAB, Ni, Co and H_2O_2 were prepared with a DiH_2O in 50mL conical tubes and filled to 50mL. 150µl of hydrochloric acid (Nacalai Tesque, 18320-15) was added to the 50mL conical DAB tube to ensure homogeneity. 800mL of 1xPBS was prepared then added to a 2L Erlenmeyer flask placed on a stir plate, the 1% DAB-NiCo solutions were added to the Erlenmeyer flask, and was homogenized with a stir rod. 350µL of 10M NaOH (AppliChem, A3910,1000) was added to bring the final pH of the DAB-NiCo to 7.1-7.4pH.

A glass basin large enough to contain 1L of liquid was used inside a fume hood and all slides within the IHC basins were manually loaded into slide racks and placed within the basin. The H_2O_2 was added to the flask just before staining to catalyze the DAB-NiCo reaction. The final working solution was poured from the flask into the basin where the slides had been placed. The incubation time (~10min) was monitored manually until the injection site could be visualized as the affected cells turned black. Manual monitoring was used to make sure that the signal-to-background noise ratio was kept from being deleterious to the final stain quality. The slides were then transferred through 3 full emersion washes of 1xPBS.

The slides were left on a drying rack overnight at RT and were put through a Giemsa counterstain after a 24-hour period. The Giemsa counterstain consisted of a 3:7 ratio of 30% Giemsa (Nacalai Tesque, 37114-35) and 70% DiH_2O, a 1xPBS wash, 1% w/v ammonium molybdate (Sigma-Aldrich, A1343-100G) wash, a second 1xPBS wash followed with ETOH dehydration. The slides were then cover-slipped and put into drying racks for 24 hours.

F. Computational Infrastructure

All of data machines within the laboratory were connected to data center using a 10g network for further analysis by a 16 node high-performance computing (HPC) cluster. Storage nodes were configured as Raid6 devices and provided 78TB of useable disk space each for a total of 156TB. The theoretical maximum transfer rate of the 10g network is 900 MB/s; however, the rate limiting process was due to the hard disk writing speed of each machine. The current average transfer speed is about 250-520MB/s.

The data processing (cropping and converting) in the data-acquisition server began when the Nanozoomer slide scanning was completed. The processed data were transferred to a central repository for quality control. This configuration could improve the overall process rate from 50% of the theoretical maximum up to 80% in performance. As shown in Figure 3, an entire network and computation pipeline setup was adopted in the RIKEN Marmoset Neural Circuit Architecture Laboratory.

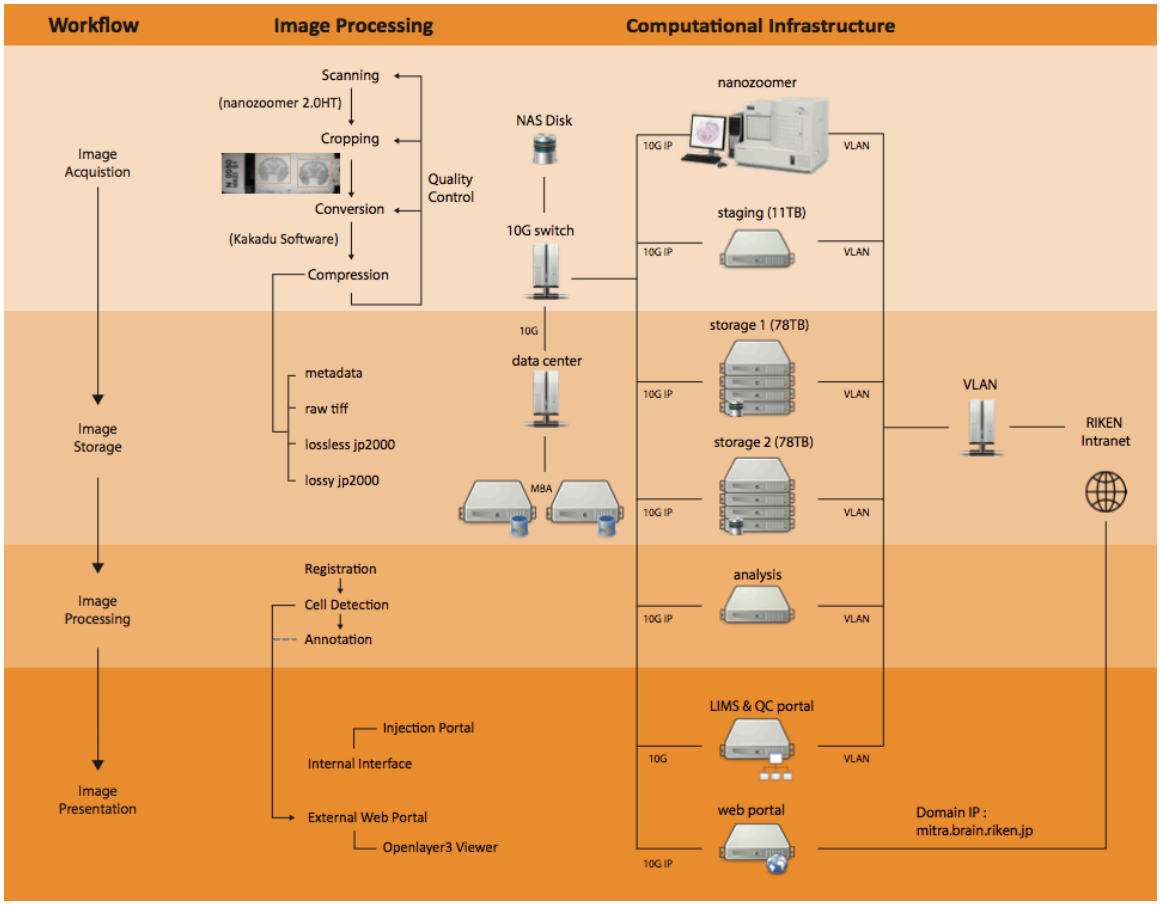

Figure 3. Computational pipeline with the network structure to perform a high-throughput data flow and process. There were four steps of workflow involved in this pipeline including image acquisition, storage, processing and presentation. With these steps, generating a whole marmoset brain dataset with high production rate and superior system performance for large data communication was possible. Each server node was connected to one 10g network for data communication and one external network for remote access.

G. Computational Processing

The computational pipeline builds upon the pipeline originally developed by the CSHL Mitra Lab for the mouse and was modified to meet the marmoset tissue size and structure (Figure 4). For each tissue section, the system produced (1) a meta-data file with all the relevant information (cropping and conversion processing); (2) a cropped ROI as a TIF format for image inspection; (3) a down sampled JPEG2000 image for rapid access for the data on the web portal; (4) an uncompressed raw data file. Our automatic detection algorithm for the cropping box placement in images performs at a 100% success rate in both brightfield and fluorescence sections. The image format used custom scripts based on the Kakadu toolkit [12]. For any given complete marmoset brain, there were a total of ~1700 sections mounted on ~900 slides.

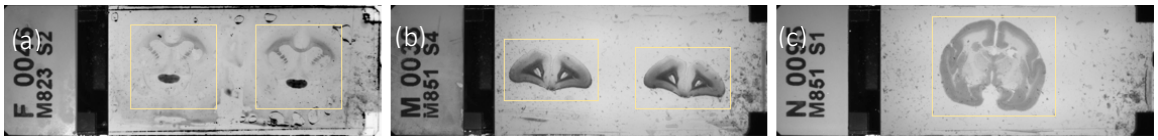

Figure 4. The Nanozoomer macro image determines the cropping ROI (a) fluorescence slide (b and c) brightfield slides shown with yellow cropping box.

This project developed and utilised an online quality control (QC) service. The QC service was employed to assess the quality of each image and determine if the re-imaging of a slide or the re-injection of an entire brain was needed. Correcting or improving the pipeline process was an evolutionary and organic process and flagging unwanted sections or materials to reduce unnecessary post-processing was a key step. The researcher had the option to view all the sections of the series (with the comparison of a micro image) and to edit the fields for QC such as tissue damage, missing sections and poor cover-slipping alignment. Once flagged, the QC service would automatically remove the sections from the dataset allowing for proper processing of the image analysis such as 2D alignment and 3D reconstruction.

The images of brain slices from histological processing were fed directly into the computational process. The post processing data involved several steps from image cropping and image conversion to 2D alignment and 3D reconstruction. This was a major departure for image analysis. Acquired image datasets were written into a propriety image format, JPEG2000. In the case of a JPEG2000 image, the decompression was ≈ 75-90 MB for fluorescence images and brightfield images (Nissl, myelin and CTB). After the proper data acquisition, automatic image processing/analysis was performed. The sections across all brains were registered into a common space. This registration was based on Nissl-stained sections for structural information and *ex-vivo* MRI as landmarks such that all sections were able to align to each other and produce a shape similar to that of the same subject reference (*ex-vivo* MRI) while maintaining coherence and continuity from section to section. A variant of the large deformation diffeomorphic metric mapping (LDDMM) algorithm was employed to compute nonlinear mapping between Brain/MINDS Nissl atlas and the reconstructed target Nissl, followed by recently developed registration methods [13].

H. Process Timeline

Based on the individual marmoset brain anterior-posterior length measured by *ex-vivo* MRI, the number of sections (20µm/section) was determined and the processing time at each step was recorded. At each step of histological processing, a small portion of brain sections were excluded from the subsequent processing based on manual quality control inspection. The final processing success rate for each series was measured by the percentage of obtained sections, shown in Figure 5.

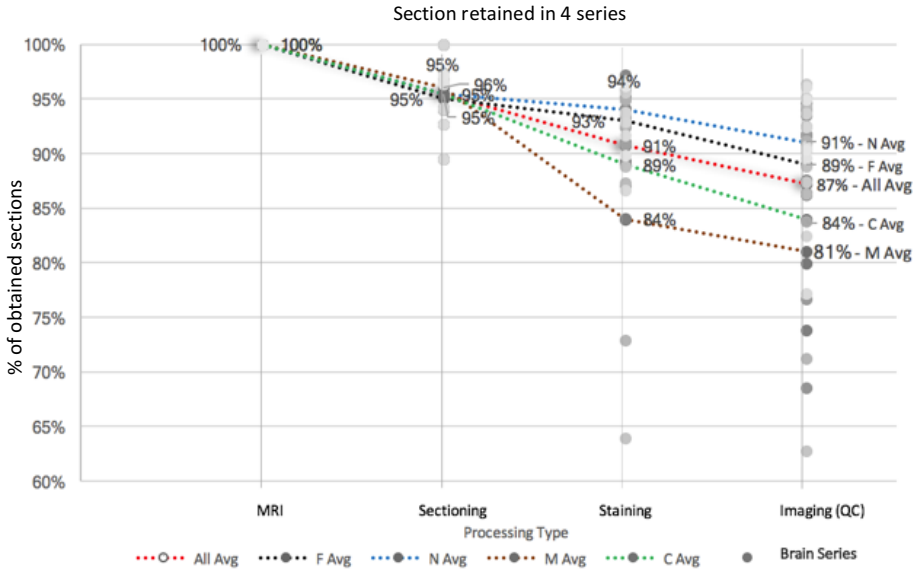

Figure 5. A pipeline processing rate with four series staining (fluorescence, Nissl, myelin, CTB) based on the latest 10 datasets. Each series starts with 100% full rate (based on the calculation from ex-vivo MRI and the number of sections needed as well as calculated by measuring at 20um each) and reduces by a percentage based on unavoidable reasons such as poor staining or section peeling. The figure shows that there is high processing rate starting with Nissl (91%), fluorescence (89%), CTB (84%), to myelin (81%). The average processing rate is 87% in total.

Reference

1 Liu, J. V., Bock, N. A. & Silva, A. C. Rapid high-resolution three-dimensional mapping of T1 and age-dependent variations in the non-human primate brain using magnetization-prepared rapid gradient-echo (MPRAGE) sequence. *NeuroImage* **56**, 1154-1163, doi:https://doi.org/10.1016/j.neuroimage.2011.02.075 (2011).

2 Hennig, J., Nauerth, A. & Friedburg, H. RARE imaging: A fast imaging method for clinical MR. *Magnetic Resonance in Medicine* **3**, 823-833, doi:10.1002/mrm.1910030602 (1986).

3 Fujiyoshi, K. *et al.* Application of q-Space Diffusion MRI for the Visualization of White Matter. *The Journal of Neuroscience* **36**, 2796 (2016).

4 Hennig, J., Nauerth, A. & Friedburg, H. *RARE imaging: A fast imaging method for clinical MR*. Vol. 3 (1986).

5 Mansfield, P. & Pykett, I. L. Biological and medical imaging by NMR. *Journal of Magnetic Resonance (1969)* **29**, 355-373, doi:https://doi.org/10.1016/0022-2364(78)90159-2 (1978).

6 Tsutomu, H., Reiko, N. & Atsushi, I. Current models of the marmoset brain. *Neuroscience Research* **93**, 116-127 (2015).

7 Mitra, P. P. The Circuit Architecture of Whole Brains at the Mesoscopic Scale. *Neuron* **83**, 1273-1283, doi:10.1016/j.neuron.2014.08.055 (2014).

8 Raspberry Pi. *Raspberry Pi Foundation*, <https://www.raspberrypi.org/> (2016).

9 Nissl., F. Ueber eine neue Untersuchungsmethode des Centralorgans zur Feststellung der Localisation der Nervenzellen. . *Neurologisches Centralblatt.* **13**, 507-508 (1894).

10 Pilati N, Barker M, Panteleimonitis S, Donga R & M., H. A rapid method combining Golgi and Nissl staining to study neuronal morphology and cytoarchitecture. . *Journal Histochem Cytochem.* **56**, 539-550 (2008).

11 Gallyas F. Silever staining of myelin by means of physical development. *Neurol Res.* **1**, 204-209 (1979).

12 Kakadu. *The world's leading JPEG2000 software development toolkit*, <http://kakadusoftware.com/> (2016).

13 Lee, B. C. *et al.* Joint Atlas-Mapping of Multiple Histological Series combined with Multimodal MRI of Whole Marmoset Brains and Quantification of Metric Distortions. *eprint arXiv:1805.04975* (2018).